Perturbative analysis of the tearing mode saturation

F. Militello, R. J. Hastie, and F. Porcelli
Burning Plasma Research Group, Department of Energetics, Politecnico di Torino, 10129 Torino, Italy

(Received 13 April 2006; accepted 18 August 2006; published online 29 November 2006)

The saturation of the tearing mode in a plasma column is investigated in the framework of the resistive magnetohydrodynamics approximation. In particular, a perturbative procedure is adopted to evaluate the structure of the magnetic island in three relevant physical conditions, depending on the model for the evolution of the resistivity, which may be affected by the growth of the mode. In cylindrical geometry, which is well suited to describe a large-aspect-ratio, low-beta tokamak plasma, the magnetic island is asymmetric with respect to the magnetic surface where reconnection occurs. New relations for the saturated island width w_s as a function of the relevant features of the equilibrium current density profile, i.e., its gradient and curvature at the reconnecting surface, are obtained. Finally, equivalent relations are also derived in the slab limit. © *2006 American Institute of Physics*. [DOI: 10.1063/1.2375036]

I. INTRODUCTION

It is well known that magnetic reconnection strongly affects the confinement and the performance of magnetic fusion experiments. The linear analysis of the tearing instability, which often develops naturally in these machines, was first investigated in the pioneering work by Furth, Killeen, and Rosenbluth.[1] However, the linear approximation, extended and generalized in many later works, breaks down when the width w of the magnetic island associated with the tearing perturbation, becomes larger than the small boundary layer around the reconnecting surface, where the effects of the electrical resistivity are relevant.

A convincing theory for the nonlinear evolution of the tearing mode, when w is small with respect to a macroscopic system length, was proposed by Rutherford,[2] and achieved a simple relation governing the growth of the island width. A key feature of the nonlinear treatment of the magnetohydrodynamic (MHD) equations in Ref. 2 is the employment of a magnetic flux surface average operator, which annihilates the convective term in the generalized Ohm's law. As a result, the velocity field is decoupled from the magnetic field evolution. A difficulty of the technique is that, in order to evaluate the flux surface averages, the knowledge of the shape of the modified magnetic surfaces is needed. In Ref. 2, analytic progress is made possible by the assumption that the constant-ψ approximation remains valid even in the nonlinear phase and that only the fundamental harmonic is excited; i.e., the structure of the magnetic island can be well represented by the linear solution. The procedure set by Rutherford has been extended in recent years to include several additional physics effects, such as neoclassical[3,4] and other kinetic effects.[5,6]

In the late nonlinear evolution of the tearing mode, the growth rate of the mode reduces gradually until the plasma achieves a new equilibrium with the saturated island. The problem of the saturation of the tearing mode is, indeed, extremely relevant in magnetic fusion research, since the presence of magnetic islands is often associated with a reduction of confinement in the new steady state plasma. The first investigation on this subject, in the low-β (=kinetic pressure/magnetic pressure) approximation, was presented by White *et al.*[7] In order to treat island saturation, the constant-ψ approximation is not accurate and a more precise knowledge of the shape of the magnetic surfaces is needed. The quasilinear treatment introduced by the authors of Ref. 7 relies on an ansatz, justified by numerical simulations, concerning the structure of the magnetic island in the neighborhood of the reconnecting surface. As in Ref. 2, it is assumed that only the dominant Fourier component of the linear mode structure plays a role in the nonlinear process. However, the application of the quasi-linear treatment to the saturation problem is questionable, and indeed the results obtained in Ref. 7 are not in agreement with numerical simulations, performed, for instance, by Biskamp in Ref. 8 (see Fig. 5.12, p. 119) and more recently by Louriero *et al.*[9] A simple and rigorous result for the "symmetric" case, which is in good agreement with the numerics, was obtained recently in Refs. 10 and 11. By symmetric case, we mean the situation where the perturbed magnetic flux has even parity as a function of the distance from the reconnecting surface. This can be realized when the gradient of the equilibrium current density vanishes at the reconnecting surface.

The nonsymmetric case, where this gradient is nonzero, is more realistic for magnetic confinement configurations of fusion interest. This case was considered by Thyagaraja,[12] who established a systematic expansion procedure, assuming $\ln(1/w) \gg 1$, so that terms of order $O(w)$ were neglected relative to terms $O[w \ln(1/w)]$. While this procedure is quite useful and indeed is at the basis of our derivation in this paper, the $O(w)$ terms neglected in Ref. 12 are important, not only from the quantitative point of view, but also because these terms guarantee the scale invariance of the final result, without which any quantitative prediction becomes impossible (see our discussion in Sec. V A). Zakharov *et al.*[13] and Pletzer and Perkins[14] corrected this problem; Zakharov *et al.* also considered the effect of finite β and of toroidal curvature. However, approximations for the island structure were still adopted in these papers and as a consequence only part of the answer was obtained.

In this paper, we present a general method for the solution of the saturation of the tearing mode that can be applied to symmetric as well as nonsymmetric islands. The new equilibrium, represented by the saturated island, is constructed using the perturbation expansion introduced by Thyagaraja[12] [but carried out to $O(w)$], which does not need an ansatz on the shape of the magnetic field, since it takes into account self-consistently the complete harmonic structure of the mode in the nonlinear layer. Our calculation is derived in both slab and cylindrical geometry, which is more pertinent to tokamak plasma modeling.

The most important results in our work concern accounting for the dependence of the resistivity $\eta \propto T^{-3/2}$ on the electron temperature profile T, which is modified by the presence of the magnetic island. In this regard, we discuss three models for the temperature, related to different physical conditions. Basically, as already pointed out by Rutherford,[2] the treatment of the island saturation problem would require an equation for the plasma temperature evolution. However, if w is small compared with a critical width $w_c \sim (\kappa_\perp/\kappa_\parallel)^{1/4}$, determined by the ratio of perpendicular over parallel thermal conductivity,[3] then the temperature profile is not changed by the presence of the island and an energy equation is not needed. In the following, we refer to this case as the first scenario or the small island case. On the other hand, if w exceeds w_c, the large thermal conductivity along the magnetic field lines leads to a flattening of the temperature profile within the island region. Furthermore, if the magnetic flux perturbation evolves rapidly on the relevant perpendicular thermal transport time scale $\tau_{\kappa_\perp}$, the global thermal equilibrium is not altered and the temperature profile shows a steep gradient on the separatrix, which becomes a discontinuity as long as only the leading order of T in w_c is concerned (second scenario or nonrelaxed large island case). This scenario is thus relevant when $\tau_\eta \ll \tau_{\kappa_\perp}$, where τ_η is the characteristic resistive time that gives a measure of the evolution time scale of the magnetic field. We recognize that, for typical plasmas produced by present day tokamaks, the perpendicular thermal diffusion time is shorter than the resistive time. Thus, the second scenario is perhaps of more academic interest, but it is nevertheless treated in this paper as it represents a useful intermediate step on the way to tackling the more realistic case, in which $\tau_\eta \gg \tau_{\kappa_\perp}$. For this latter case, the island evolves slowly on the thermal diffusion time scale and the jump in temperature is smoothed away, assuring continuity of the temperature on the whole domain. If the conditions at the plasma edge (i.e., the scrape-off layer) maintain the temperature efficiently, and there is only a heat source in the core plasma, it follows that the presence of the island results in the cooling of the core itself. We call this last physical situation the third scenario or relaxed large island case.

For the relatively small islands of the first scenario, i.e., $w \ll w_c$, our results correct and extend rigorously those in previous literature, which gave only approximate answers. Furthermore, we detail here the derivation of the second scenario (nonrelaxed large island case), whose final result has already been presented in Ref. 15. The third scenario, where the resistivity profile is modified by relatively large islands and the temperature is continuous across the separatrix at every order, is considered in this paper for the first time, to our knowledge.

The paper is organized as follows. In Sec. II, the mathematical model is introduced. A description of the asymptotic matching technique employed to solve the nonlinear MHD equations is described in Sec. III. The three physical regimes under investigation and their limits of validity are detailed in Sec. IV, while the derivation of their saturation relations is presented in Sec. V. In Sec. VI, similar relations are given in the case of slab geometry. Finally, in Sec. VII, we summarize the results obtained and we draw our conclusions.

II. MODEL EQUATIONS

The mathematical model that we adopt is well suited to describe a single helicity tearing mode that grows in a low-beta, large-aspect-ratio tokamak and whose width is small as compared to the macroscopic length scale. Thus, the calculations that we present are based on a two-dimensional cylindrical approximation. Assuming that the system possesses helical symmetry, it is useful to introduce an helical coordinate, i.e., $\xi = \vartheta - (n/mR)z$, where ϑ is the poloidal coordinate, m and n the poloidal and toroidal mode numbers, respectively, and R the equivalent major radius of the tokamak. Thus, the magnetic field and the plasma velocity configuration can be expressed as

$$\mathbf{B} = B_T \mathbf{e_z} + \nabla\Psi \times \mathbf{e_z}, \tag{1}$$

$$\mathbf{V} = V_T \mathbf{e_z} - \nabla\Phi \times \mathbf{e_z}, \tag{2}$$

where Ψ and Φ represent a magnetic flux function and a stream function, respectively. $B_T \approx$const is the value of the strong confining magnetic field in the direction along the cylinder axis, specified by the unit vector $\mathbf{e_z}$, and V_T is the plasma velocity along the same direction.

The initial Ohmic equilibrium is supposed given and specified by the functions $\Psi_{\text{eq}} = \psi_{\text{eq}}(r)$, $\Phi_{\text{eq}} = 0$, and $V_{T,\text{eq}} = 0$. Since the perturbed configuration has helical symmetry, it is possible to find a direction along which the magnetic field does not play a role in the reconnection process. The projection of the magnetic field along this direction, denoted by $\mathbf{B_c} = B_z \mathbf{e_z} - (rnB_T/Rm)\mathbf{e}_\theta$, is identified by the condition that $\mathbf{k}\cdot\mathbf{B_c} = 0$ everywhere, with $\mathbf{k}$ the mode wave vector. Therefore, the coordinate perpendicular to r and ξ may be ignored, and the problem is two-dimensional. The residual part of $\mathbf{B}$ is the sheared magnetic field, $\mathbf{B}_* = \mathbf{B} - \mathbf{B_c} = \nabla\Psi_* \times \mathbf{e_z}$, which reverses its direction around the neutral line, i.e., at $r = r_s$, where reconnection takes place. The reconnecting surface is where the magnetic winding number (safety factor), $q(r) = rB_T/RB_P$, is equal to the ratio m/n, with B_P the equilibrium poloidal magnetic field. The perturbation of the magnetic flux can also be described in a functional way by splitting:

$$\Psi(r,\xi) = \Psi_*(r,\xi) - \frac{r^2 n B_T}{2mR}, \tag{3}$$

where ψ and ψ_* are the perturbed poloidal and helical magnetic flux functions, respectively. The current density flowing in the direction of the axis of the plasma column is related to the helical magnetic flux function through Ampère's law, $J=-\nabla_\perp^2\Psi_*+2nB_T/Rm=-\nabla_\perp^2\Psi$, where $\nabla_\perp^2 f=r^{-1}\partial_r(r\partial_r f)+r^{-2}\partial_\xi^2 f$ and $J_*=-\nabla_\perp^2\Psi_*$ is the helical current density.

In the following, the radial coordinate r is normalized with respect to R, the time to the relevant Alfvén time, and B_T is taken equal to unity. A reduced version of the MHD equations is used to describe the physics of the problem. It can be shown that perturbations of V_T and B_T are negligibly small in the low-β, strong magnetic guide field regime relevant to tokamak plasmas. Introducing Ψ_*, the plasma vorticity equation in cylindrical geometry becomes

$$\frac{\partial U}{\partial t} + [\Phi, U] = [J, \Psi_*], \tag{4}$$

where $U=\nabla_\perp^2\Phi$ is the vorticity and the operator $[f,g]=r^{-1}(\partial_r f\partial_\xi g-\partial_r g\partial_\xi f)$ is the Poisson bracket in cylindrical coordinates. Equation (4) is coupled with the z component of Ohm's law:

$$\frac{\partial \Psi_*}{\partial t} + [\Phi, \Psi_*] = E_z - \eta(T)J, \tag{5}$$

E_z is the constant electric field along the direction z, which, in a tokamak, corresponds to the induced toroidal electric field, that balances the term $\eta_{\text{eq}}(r)J_{\text{eq}}(r)$ at equilibrium.

The local features of the equilibrium current density strongly affect the final saturated state of the mode, as will be shown in the following. In particular, it will be useful to Taylor expand $J_{\text{eq}}(r)$ in the neighborhood of the reconnecting surface r_s:

$$\frac{J_{\text{eq}}(x)}{J_{\text{eq}}(0)} = 1 + a_s x + b_s\frac{x^2}{2} + O(x^3), \tag{6}$$

where $x=(r-r_s)/r_s$ is a dimensionless measure of distance from the resonant surface. Thus, henceforth the equilibrium will be simply characterized by the parameters $a_s=r_sJ'_{\text{eq}}(0)/J_{\text{eq}}(0)$ and $b_s=r_s^2J''_{\text{eq}}(0)/J_{\text{eq}}(0)$, where the prime stands for derivative with respect to r.

In Eq. (5), the resistivity is assumed to be a function of the electron temperature, following the standard Spitzer expression for the fully ionized plasma, $\eta\propto T^{-3/2}$. Therefore, an equation for the temperature evolution is required to close the problem. Assuming that reconnection involves a region of the plasma far from both the scrape-off layer and the core, heat transport is the dominant process in the temperature evolution (i.e., it is reasonable to neglect heat sources or sinks):[3]

$$\nabla_\parallel \kappa_\parallel \nabla_\parallel T + \nabla_\perp \cdot \kappa_\perp \nabla_\perp T = 0, \tag{7}$$

where $\kappa_\parallel$ and $\kappa_\perp$ are the anisotropic components of the thermal conductivity and $\nabla_\parallel=(\mathbf{B}\cdot\nabla)/B$. If $\kappa_\perp$ were classical, it would be a function of the temperature and its profile would be affected by the presence of the island in the same way as that of η. However, the perpendicular electron thermal diffusivity in fusion devices is anomalous. This behavior is probably determined by the electrostatic turbulence of trapped electron modes and ion temperature gradient modes. These may respond to temperature gradients, but the most natural and simplest assumption is that $\kappa_\perp=\kappa_\perp(r)$ remains a function of r in the presence of the island. Typically, in a magnetically confined plasma, the parallel thermal transport is much more efficient than the perpendicular one, i.e., $\kappa_\perp\ll\kappa_\parallel$, so that the effect of the perpendicular term in Eq. (7) is relevant only over length scales of order $w_c\sim(\kappa_\perp/\kappa_\parallel)^{1/4}\ll 1$. Finally, we remark that the equilibrium current profile $J_{\text{eq}}(r)$ can be related to the equilibrium temperature profile $T_{\text{eq}}(r)$, since we assume a steady state in which the inductive electric field is constant. Thus, $J_{\text{eq}}(r)\propto T_{\text{eq}}^{3/2}(r)$, and it follows that $a_s=(3/2)r_sT'_{\text{eq}}(0)/T_{\text{eq}}(0)$ and $b_s-a_s^2/3=(3/2)r_s^2T''_{\text{eq}}(0)/T_{\text{eq}}(0)$.

III. MATCHING PROCEDURE

Although the problem of the saturation of the tearing mode is fundamentally nonlinear, it can be simplified when the island width is much smaller than a macroscopic equilibrium scale length L. In this case, the dissipation and nonlinearities are relevant only in a narrow layer around the reconnecting surface of width $\delta\sim w$, while everywhere else a linear approximation is essentially adequate (apart from a small correction discussed in Sec. V A). Thus, it is possible to calculate separately a linear outer region and a nonlinear inner layer, whose smallness allows geometrical simplifications, and then match the solutions in the region where they overlap. The final goal of the matching procedure is to obtain an equation relating the features of the equilibrium current density with the saturated island width: $w_s=w_s(a_s,b_s,s,A,\Delta')$, where A is the parameter that characterizes the global asymmetry of the mode (see Refs. 16 and 17) and $s=(d\ln q/d\ln r)_{r_s}$ is the magnetic shear parameter at the reconnecting surface. We remark that the smallness of the island size can be assured by the choice of an equilibrium such that, upon restoring the normalization scale, $\Delta' L\sim w/L$. This means that the range of validity of our calculation is restricted by the constraint $\Delta' L\leq 1$. In this regard, we remark that our calculation does not apply to the $m=1$ mode.

In the outer region, it is convenient to express the perturbed magnetic flux through its Fourier representation: $\psi_*=\Sigma\tilde{\psi}_{*m}(r,t)e^{im\xi}$. Thus, each $\tilde{\psi}_{*m}$ is described by the linearized equation

$$\frac{1}{r}\frac{\partial}{\partial r}r\frac{\partial\tilde{\psi}_*}{\partial r} - \left(\frac{m^2}{r^2} + \frac{\dfrac{1}{r}\dfrac{d\hat{J}_{\text{eq}}}{dr}}{\dfrac{1}{q_{\text{eq}}} - \dfrac{n}{m}}\right)\tilde{\psi}_* = 0, \tag{8}$$

which is obtained from Eq. (4), neglecting inertia and identifying $\tilde{\psi}_{*m}$ with $\tilde{\psi}_*$. In Eq. (8), $\hat{J}_{\text{eq}}=RJ_{\text{eq}}/B_T$ is the dimensionless current density. In the vicinity of the reconnecting surface, Eq. (8) can be expanded:

$$\frac{\partial^2 \tilde{\psi}_*}{\partial x^2} + (1-x)\frac{\partial \tilde{\psi}_*}{\partial x} - \left(m^2 + b - \frac{a^2}{2} + \frac{a}{2} + \frac{a}{x}\right)\tilde{\psi}_* = 0, \quad (9)$$

with $a=a_s(1-2/s)$ and $b=b_s(1-2/s)$. Note that $\psi_*(x)$ does not have a definite parity as a function of x, because in general $d\hat{J}_{\rm eq}/dx$ does not vanish at the reconnecting surface.[16,17] A local solution of Eq. (9) can be expressed through a series expansion:[16]

$$\tilde{\psi}^{\pm}_{*\rm out} = \left\{ 1 + ax\ln(|x|) + (a^2 - a)\frac{x^2}{2}\ln(|x|) + \frac{\hat{k}^2 x^2}{2} + \cdots \right. \\ \left. + \frac{A \pm \Delta'}{2}\left[x + \frac{(a-1)x^2}{2} + \cdots\right]\right\}\psi_{*0}, \quad (10)$$

where $\hat{k}^2=m^2+b+a-2a^2$. The term involving $(A\pm\Delta')$ contains the asymptotically small solution on either side of the resonance, together with the term $-ax$ from the large solution. With the transformation $A\to\hat{A}-2a$, the terms labeled by $(\hat{A}\pm\Delta')$ separate off and label the small solution. The solution has two branches: $\tilde{\psi}^{-}_{*out}$ for $x<0$ and $\tilde{\psi}^{+}_{*\rm out}$ for $x>0$. We have chosen ψ_{*0} so that the expansion (10) is continuous at $r=r_s$, with ψ_{*0} an arbitrary amplitude. This will be required by the matching to the island region in scenarios 1 and 2, but will be relaxed in Sec. VI when we consider scenario 3. The parameters A and Δ' depend on the global features of the equilibrium current density profile and on the mode wave vector and, in general, can be evaluated numerically. The magnetic island associated with this perturbation is asymmetric with respect to the reconnecting surface if either of the constants a or A is different from zero and has a width $w\cong 4\sqrt{\psi_{*0}/J_{*eq}(0)}$. It is convenient to introduce a matching function M whose limit for $x\to 0$ is the standard linear stability parameter Δ':[1]

$$M(x) = \frac{1}{\psi_{*0}}\left(\left.\frac{\partial\tilde{\psi}_*}{\partial x}\right|_x - \left.\frac{\partial\tilde{\psi}_*}{\partial x}\right|_{-x}\right), \quad \Delta' = \lim_{x\to 0} M(x). \quad (11)$$

Hence, using the solution (10), we find in the outer region,

$$M_{\rm out}(X) = \Delta' + 2wX\left\{(a^2-a)\ln|X| \right. \\ + \left[(a-1)\left(\frac{A}{2} + a\ln w\right) + m^2 + b - \frac{3}{2}a^2 \right. \\ \left.\left. + \frac{1}{2}a\right]\right\} + O(w^2\ln w), \quad (12)$$

where $X=x/w$.

The solution in the inner layer can be obtained by extending the standard procedure introduced by Rutherford for the nonlinear evolution of the tearing mode.[2] In the nonlinear layer the model equations can be reduced to a simpler version. In particular, it can be shown that the stream function is of order η as compared to Ψ_*, so that the inertial terms in Eq. (4), i.e., $[\Phi,U]$, can be neglected. Consequently, the current density becomes a function of the helical flux only; i.e., $J=J(\Psi_*)$. Similarly, Φ can be eliminated in Ohm's law by annihilating the Poisson bracket term. This is done by applying to Eq. (5) the averaging operator $\langle f\rangle$, defined as

$$\langle f\rangle = \frac{\left(\oint \left|\frac{\partial\Omega}{\partial X}\right|^{-1} f d\xi\right)}{\left(\oint \left|\frac{\partial\Omega}{\partial X}\right|^{-1} d\xi\right)}, \quad (13)$$

with $\Omega=[\psi_{*\rm eq}(0)-\Psi_*(X,\xi)]/\psi_{*0}$, a conveniently normalized flux variable. The integration $\oint d\xi$ is taken over $[-\pi,\pi]$ for "open" flux surfaces outside the island separatrices (i.e., $\Omega>1$) and between zeros of $\partial\Omega/\partial X$ for "closed" magnetic surfaces within the island. (i.e., for $-1<\Omega\leq 1$). This operator is such that $\langle[f,\Psi_*]\rangle=0$, if the function f is periodic in ξ. A further simplification is the neglect of time derivatives, since we are interested in the saturation regime. As a result, we find from Eq. (5) that the total current density along z in the inner layer may be written as

$$J_{\rm in}(\Psi_*) = \frac{E_z}{\langle\eta\rangle}. \quad (14)$$

The nonlinear current density $J_{\rm in}$ determines the matching function in the inner region:

$$M_{\rm in}(X) = -\frac{w}{\pi\psi_{*0}}\int_{-X}^{X} dX'\int_0^{2\pi} d\xi\cos\xi \\ \times\left(J_{\rm in} + \frac{w^{-1}}{1+wX}\frac{\partial\Psi_{*\rm in}}{\partial X} + \frac{\partial^2\Psi_{*\rm in}}{\partial\xi^2}\right). \quad (15)$$

Note that $J^*_{\rm in}=J_{\rm in}-2n/m$, but the constant term $2n/m$ does not contribute to the integral. Thus, in Eq. (15) we have substituted the helical current density with $J_{\rm in}$, since, under the integral, they give an equivalent result. In order to have the expression above completely determined, a model for the resistivity is required.

IV. RESISTIVITY MODELS

In the first scenario (the "small island" case, $w\ll w_c$), the resistivity profile is not modified significantly by the presence of the island, as can be recognized by the inspection of Eq. (7). Hence, $\eta=\eta_{\rm eq}(r)$ also in the nonlinear evolution. By expanding $\eta_{\rm eq}$ around the resonant surface in Eq. (14), we obtain an expression for the current $J_{\rm in}$ in the inner layer up to order w^2:

$$\frac{J_{\rm SI}(\Psi_*)}{J_{\rm eq}(0)} = 1 + wa_s\langle X\rangle + w^2(b_s - 2a_s^2)\left\langle\frac{X^2}{2}\right\rangle + w^2a_s^2\langle X\rangle^2 \\ + \cdots, \quad (16)$$

where the subscript "SI" refers to the small island case.

In the second scenario (the "nonrelaxed large island" limit, $w\gg w_c$ and $\tau_\eta\ll\tau_{\kappa_\perp}$) the outer equilibrium is unaltered and the temperature in the neighborhood of the island is matched onto the original equilibrium temperature $T_{\rm eq}(x)$, on both sides of the island (see Fig. 1). For the calculation of the electron temperature, it is also possible to split the problem and identify a linear outer region, where the perturbation of the magnetic flux induces a self-consistent antisymmetric

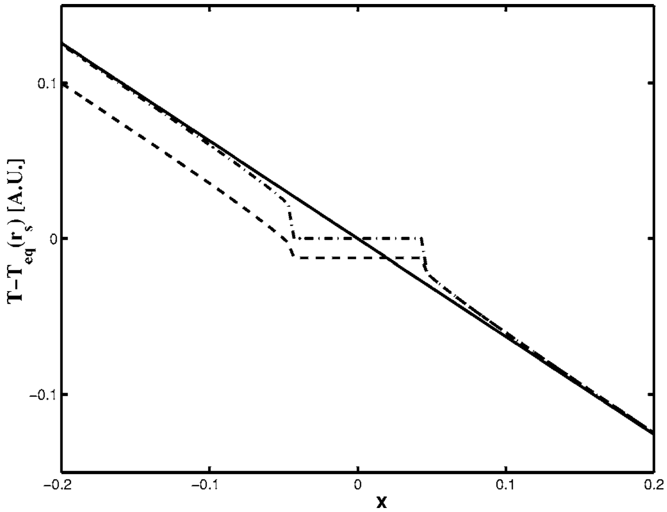

FIG. 1. Temperature profiles in a poloidal cross section passing through the O-point of the magnetic island, as a function of the distance x from the resonant surface. The solid line is the equilibrium profile (valid also for the first scenario), the dash-dotted line is the second scenario profile, and the dashed line refers to the third scenario.

perturbation of the temperature, and an inner region, where T is obtained by solving Eq. (7). Since $w \gg w_c$, an initial expansion of T in powers of w_c/w shows that the temperature, and consequently the resistivity, are functions of the helical flux function only: $\eta = \eta(\Psi_*)$. Indeed, to the lowest order in w_c, the second term on the right-hand side of Eq. (7) can be neglected. Accordingly, the thin thermal boundary layer produced by the perpendicular transport around the separatrix is neglected. A discussion of the boundary layer and of the path around the island followed by heat diffusing from the core to the plasma edge has been given by Fitzpatrick.[3] In addition, as a consequence of the antisymmetry of the boundary conditions, in the region inside the separatrix ($\Omega < 1$), the temperature profile is flattened and the resistivity is almost constant. On the other hand, outside the island ($\Omega > 1$), the temperature profile can be found by the integration of the solubility condition of Eq. (7):[2,3]

$$\frac{d}{d\Omega}\left(\frac{dT}{d\Omega}\int r\kappa_{\perp}(r)|\partial_X \Omega| d\xi\right) = 0, \tag{17}$$

which can be derived by averaging Eq. (7) over Ω and observing that $T = T(\Omega)$, to the lowest order in the w_c/w expansion. The observations above imply that, in this limit, $J_{\text{in}}(\psi_*)$ in Eq. (14) can be written as

$$\frac{J_{\text{LI}}(\Psi_*)}{J_{\text{eq}}(0)} = \frac{T^{3/2}(\Psi_*)}{T_{\text{eq}}^{3/2}(r_s)} = \frac{T_0^{3/2}}{T_{\text{eq}}^{3/2}(r_s)} \times\left[1 + w\frac{3}{2}\frac{T_1}{T_0} + w^2\left(\frac{3}{2}\frac{T_2}{T_0} + \frac{3}{8}\frac{T_1^2}{T_0^2}\right) + \cdots\right], \tag{18}$$

where the temperature has been expanded in the useful form: $T(\Omega) = T_0 + wT_1(\Omega) + w^2 T_2(\Omega) + \cdots$, and the subscript "LI" denotes that this applies to the large island case.

The third scenario (the "relaxed large island" limit, $w \gg w_c$ and $\tau_\eta \gg \tau_{\kappa_\perp}$) is similar to the second scenario, but it applies if thermal relaxation occurs before island saturation. The model could also apply if $\tau_\eta \ll \tau_{\kappa_\perp}$, but after a long enough time has passed; i.e., $t \gg \tau_{\kappa_\perp}$. This implies that the steep temperature gradients at the separatrix of the island have disappeared, inducing a drop of the temperature in the core of the plasma ($x < 0$) and, consequently, a degradation of confinement.[18] Therefore, the local smoothing of the temperature profile is responsible for a global relaxation (see Fig. 1). Indeed, the reduction of T in the core would also cause a drop of the current density for $X < 0$ [cf. Eq. (14)]. Consequently, the inductive electric field will have to increase to maintain a constant plasma current, $I = \int_0^a r dr \oint d\xi J(\Omega)$, thus increasing the current density for $X > 0$. Both the linear outer solution and the nonlinear inner solution are modified by these perturbations of the equilibrium. The current density J_{in} in the inner layer is

$$\frac{J_{\text{RLI}}(\Psi_*)}{J_{\text{eq}}(0)} = \frac{(E_z + \Delta E)(T + \Delta T)^{3/2}}{E_z T_{\text{eq}}^{3/2}(r_s)}, \tag{19}$$

where $T(\Omega)$ is the same as in Eq. (18), $\Delta T \equiv \text{const}$ is the drop in temperature within the island (see the next section), and ΔE is the increase in the inductive electric field required to maintain the original plasma current I. The structure of the global perturbations induced in the "nonrelaxed large island" model by the relaxation of the gradients of T on the separatrix ΔE and ΔT, will be reviewed and analyzed in the Sec. VII.

V. ANALYTIC EXPRESSION FOR THE SATURATED ISLAND WIDTH

In this section, we derive the saturated island width for the three scenarios outlined in the previous section.

A. First scenario: The small island case

The magnetic structure of the "small island" ($w \ll w_c$) can be obtained self-consistently from Eq. (16) using Ampère's law. Note that Eq. (16) can be seen as a difficult integro-differential equation, whose unknown is the function $\Omega(X,\xi)$. In order to calculate the normalized magnetic flux, an expansion of J and Ω in powers of w can be employed:

$$\Omega(X,\xi) = \Omega_0 + w\Omega_1 + w^2\Omega_2 + \cdots, \tag{20}$$

$$J_{\text{in}}(\Omega) \equiv J_{\text{SI}}(\Omega) = J_0 + wJ_1 + w^2 J_2 + \cdots, \tag{21}$$

such that the problem, order by order, is reduced to a set of simpler equations. An important feature of this system of equations is that the solution for $J(\Omega)$, at any given order, requires a knowledge of only the flux surface shape, i.e., of $\Omega(X,\xi)$, to one order less in the expansion.[12,15] Starting from the lowest order equation, an iterative procedure permits a complete solution of the problem. The equations are

$$\frac{\partial^2\Omega_0}{\partial X^2} = 16\frac{J_{*0}}{J_{\mathrm{eq}*}(0)} = 16, \tag{22}$$

$$\frac{\partial^2\Omega_1}{\partial X^2} = 16\frac{J_{*1}}{J_{\mathrm{eq}*}(0)} = 16a\langle X\rangle_0 - \frac{1}{r_s}\frac{\partial\Omega_0}{\partial X}, \tag{23}$$

$$\frac{\partial^2\Omega_2}{\partial X^2} = 16\frac{J_{*2}}{J_{\mathrm{eq}*}(0)} = \cdots,$$

where the zero-order average $\langle X\rangle_0$ is defined in Appendix A, and we recall that $J_*=J-2n/m$. The boundary conditions at large values of X, for these equations involve matching to the linear solution in the outer region [see Eq. (10)]. For the purposes of this calculation, it is sufficient to calculate Ω up to order w. Thus, from Eq. (22), Ω_0 defines the lowest-order, symmetric structure of the island, corresponding to the constant-ψ approximation used in Refs. 2 and 3:

$$\Omega_0 = 8X^2 - \cos\xi. \tag{24}$$

At the next order, i.e., Ω_1, which describes the asymmetries of the island, is obtained from Eq. (23) upon integration by parts:

$$\begin{aligned}\Omega_1 = \sigma Ha\Bigg[&\frac{\sqrt{2}}{12}\Omega_0^{3/2} + \frac{\sqrt{2}}{4}\sqrt{\Omega_0}\cos\xi \\ &- \frac{\sqrt{2}}{8}\cos\xi\sqrt{\Omega_0+\cos\xi}\ln w \\ &\times\left(\frac{\Omega_0}{16} + \frac{\cos\xi}{32} + \frac{\sqrt{\Omega_0}\sqrt{\Omega_0+\cos\xi}}{16}\right)\Bigg] \\ &- \left(\frac{A}{2} + a\ln w + \frac{a}{2}\right)X\cos\xi - \frac{8}{3}\frac{X^3}{r_s} \\ &+ aXG_1(\Omega,\xi) - \sigma HaG_2(\Omega),\end{aligned} \tag{25}$$

where $\sigma=|X|/X$, $H=H(\Omega-1)$ is the Heaviside function, equal to 0 inside the separatrix and to 1 outside, G_1 and G_2 are defined in Appendix A. It should be noted that integrating up Eq. (23) in the three regions (outside the separatrix, i.e., $X<0$ and $X>0$, and within the island), introduces six arbitrary functions; i.e., $C_j(\xi)$. Continuity of $\partial\Omega/\partial X$ and Ω at the separatrix reduces these to two, which are then determined by matching to the linear eigenmode in the outer region, $|X|\gg 1$. Surprisingly, this leaves a part of Ω_1 [G_2 in Eq. (25)], which does not match to either the equilibrium flux in the outer region or the linear perturbed flux. The unmatched part of Ω_1 is of odd parity in σ and is constant ($\sim 0.37\sigma$) in the $X\to\infty$ limit. When expressed in global outer variables, it is of magnitude $O(w^3)$ relative to the equilibrium. It therefore appears that reconnection in the inner region is responsible for driving a nonlinear modification of the outer equilibrium, but since this is $O(w^3)$, it will have a negligible effect on mode saturation.

It is now possible to evaluate the average operators in Eq. (16) up to order w^2 (see Appendix A). Therefore, after the substitution of J_{SI} in Eq. (15), M_{in} is also completely determined up to order w^2. For the sake of brevity, the mathematical details of this calculation are reported in Appendix A. The inner matching function can be asymptotically matched to M_{out} in the overlapping region, i.e., $w\ll x\ll 1$, thus giving an expression for the saturated island size w_s:

$$\begin{aligned}\Delta' = 0.41w_s\Bigg\{&a^2\left[\ln\left(\frac{1}{w_s}\right) + 4.85 - \frac{0.68}{2-s}\right] \\ &- \frac{Aa}{2} - b - 0.44a\Bigg\}.\end{aligned} \tag{26}$$

We remark that the logarithmic term in Eq. (26) has been obtained in a previous investigation by Thyagaraja,[12] using a similar mathematical technique. The key difference between Ref. 12 and our calculation lies in the precision of the determination of the structure of the island. Indeed, in Ref. 12, the $w\ln w$ term in (25) is assumed to be of lower order with respect to the other $O(w)$ terms, which are therefore neglected. This approximation significantly simplifies the evaluation of the average operators in Eq. (16), but, at the same time, restricts the validity of the calculation to smaller islands [cf. Eq. (26)]. Finally, note that the combination $\ln(1/w_s)-0.5A/a$ does not depend on the choice of the normalization length L.

B. Second scenario: The nonrelaxed large island case

In this scenario, in order to obtain the relation for the saturated island width, the evaluation of the temperature profile modified by the island is required [cf. Eqs. (15) and (18)]. As we pointed out previously, when the island is large, the temperature inside the separatrix becomes approximately constant and equal to the equilibrium value at the reconnecting surface, i.e., $T=T_{\mathrm{eq}}(r_s)+w^2T_2(\Omega)$. In the nonlinear region outside the island, Eq. (17) must be solved. In Refs. 2 and 3, one can find a solution of this equation, accurate to order w. However, for our purposes, corrections of order w^2 involving $T_2(\Omega)$ are needed. Noting that $\kappa'_\perp(r_s)/\kappa_\perp(r_s)+r_s^{-1} = -T''_{\mathrm{eq}}(r_s)/T'_{\mathrm{eq}}(r_s)$, where the prime represents a differentiation with respect to r, we obtain to order w^2

$$\frac{dT}{d\Omega} = w\frac{\sigma 2\pi T'_{\mathrm{eq}}(r_s)}{\displaystyle\int_0^{2\pi} d\xi\frac{\partial\Omega}{\partial X}} + w^2\frac{\displaystyle 2\pi T''_{\mathrm{eq}}(r_s)\int_0^{2\pi} d\xi X\frac{\partial\Omega}{\partial X}}{\displaystyle\left(\int_0^{2\pi} d\xi\frac{\partial\Omega}{\partial X}\right)^2} + O(w^3). \tag{27}$$

To find the solution of this equation, it is again possible to employ a perturbative procedure. As in the small island case, the calculation of T_1 (and hence J_1) requires a knowledge of only the lowest-order flux function $\Omega_0(X,\xi)$. The system of equations is

$$\frac{dT_0}{d\Omega} = 0, \tag{28}$$

$$\frac{dT_1}{d\Omega} = \frac{\sigma 2\pi T'_{\mathrm{eq}}(r_s)}{\displaystyle\int_0^{2\pi} d\xi \left.\frac{\partial\Omega}{\partial X}\right|_0}, \tag{29}$$

$$\frac{dT_2}{d\Omega}=\frac{2\pi T''_{\mathrm{eq}}(r_s)\int_0^{2\pi}d\xi X\left.\frac{\partial\Omega}{\partial X}\right|_0}{\left(\int_0^{2\pi}d\xi\left.\frac{\partial\Omega}{\partial X}\right|_0\right)^2}-\frac{\sigma 2\pi T'_{\mathrm{eq}}(r_s)\int_0^{2\pi}d\xi\left.\frac{\partial\Omega}{\partial X}\right|_1}{\left(\int_0^{2\pi}d\xi\left.\frac{\partial\Omega}{\partial X}\right|_0\right)^2},\tag{30}$$

where $\partial_X\Omega|_0=4\sqrt{2}\sqrt{\Omega+\cos\xi}$ and $\partial_X\Omega|_1=\partial_X\Omega_1-\Omega_1/X$. For this case, the global thermal equilibrium is not altered by the presence of the island (see Fig. 1). It follows that the boundary conditions for Eqs. (28)–(30) are specified by the temperature profile in the linear outer region, i.e., $T_{\mathrm{out}}=(J_{\mathrm{out}}/CE_z)^{2/3}$, where C is a constant of proportionality.

In parallel with this set of equations, the following system must be solved:

$$\frac{\partial^2\Omega_0}{\partial X^2}=16,\tag{31}$$

$$\frac{\partial^2\Omega_1}{\partial X^2}=16a\frac{T_1}{T'_{\mathrm{eq}}(r_s)}-\frac{1}{r_s}\frac{\partial\Omega_0}{\partial X},\qquad \frac{\partial^2\Omega_2}{\partial X^2}=\cdots.\tag{32}$$

This is a perturbative expansion of Ampère's equation and (14), whose solutions are used to evaluate the right-hand side of (29) and (30). We then find that the zero-order temperature takes the constant value $T_0=T_{\mathrm{eq}}(r_s)$, and that the zero-order, symmetric normalized flux is equivalent to that in the small island case: Eq. (24). To the next order, the solution of Eq. (29) in integral form is

$$T_1(\Omega)=-\frac{\sigma H\sqrt{2}T'_{\mathrm{eq}}(r_s)}{8}\int_\Omega^\infty d\Omega'\left[\frac{\pi}{2\sqrt{\Omega'+1}E(m')}-\frac{1}{\sqrt{\Omega'}}\right]+\sigma HT'_{\mathrm{eq}}(r_s)\frac{\sqrt{2}}{4}\sqrt{\Omega},\tag{33}$$

where $E(m')$ is the elliptic integral of the second kind and $m'=2/(\Omega'+1)$. A peculiar feature of T_1 is that it takes a value different from zero for $\Omega=1$, so that, in the nonrelaxed large island model, a discontinuity of the temperature appears on the separatrix, as shown in Fig. 2. We remark that, in principle, the continuity of T could be recovered by taking into account a thermal boundary layer around the separatrix where the perpendicular transport is relevant; i.e., by obtaining a higher-order solution in $\kappa_\perp/\kappa_\parallel$. Physically, the discontinuity would then be replaced by a steep gradient in the temperature profile in the neighborhood of the surface $\Omega=1$. Now, Eq. (32) is completely determined and can be solved for $\Omega_1(X,\xi)$:

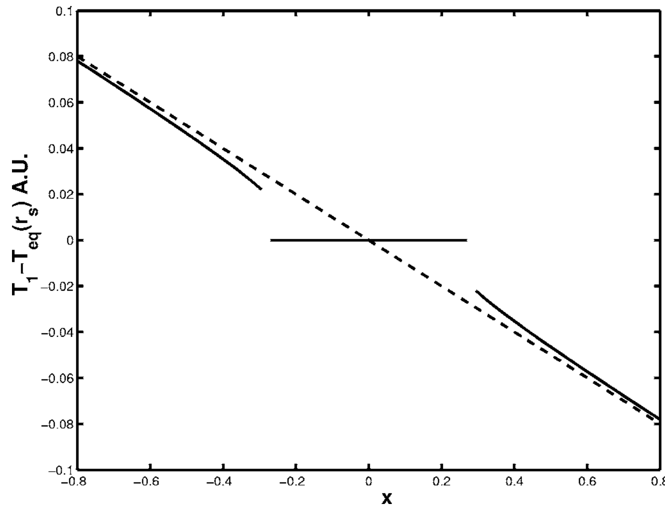

FIG. 2. Profile of T_1 in a poloidal cross section passing through the O-point of the magnetic island (solid line), as a function of the distance from the resonant surface, x. The dashed line is the equilibrium profile. Note the discontinuity at the separatrix.

$$\Omega_1=\sigma Ha\left[\frac{\sqrt{2}}{12}\Omega_0^{3/2}+\frac{\sqrt{2}}{4}\sqrt{\Omega_0}\cos\xi-\frac{\sqrt{2}}{8}\cos\xi\sqrt{\Omega_0+\cos\xi}\ln\left(\frac{\Omega_0}{16}+\frac{\cos\xi}{32}+\frac{\sqrt{\Omega_0}\sqrt{\Omega_0+\cos\xi}}{16}\right)\right]-\left(\frac{A}{2}+a\ln w+\frac{a}{2}\right)X\cos\xi-\frac{8}{3}\frac{X^3}{r_s}+aXF_1(\Omega,\xi)-\sigma HaF_2(\Omega),\tag{34}$$

with the functions F_1 and F_2 defined in Appendix B, similarly to G_1 and G_2. In this case as well, Ω_1 contains an unmatched part, due to F_2, which is odd in X, which approaches a constant value far from the reconnecting surface. As in the first scenario, this term is $O(w^3)$, so its effect on the outer equilibrium can be neglected. Finally, we calculate T_2, by integrating Eq. (30):

$$T_2=-H\left(\frac{T''_{\mathrm{eq}}(r_s)}{16}+\frac{T'_{\mathrm{eq}}(r_s)}{48}\right)\int_\Omega^\infty d\Omega'\left[\frac{\pi^2\Omega'}{4E^2(\Omega'+1)}-1\right]-H\frac{T'_{\mathrm{eq}}(r_s)a}{48}\int_\Omega^\infty d\Omega'\left\{\frac{3\pi\sqrt{2}K}{2E^2(\Omega'+1)^{3/2}}\times\left[\frac{\sqrt{2}}{6}(\Omega'^{3/2}-1)+\frac{\sqrt{2}\pi}{8}\int_1^{\Omega'}d\Omega''\hat{F}(\Omega'')\right]+1\right\}+H\frac{T''_{\mathrm{eq}}(r_s)}{16}\Omega+H\frac{T'_{\mathrm{eq}}(r_s)}{48}\Omega-H\frac{T'_{\mathrm{eq}}(r_s)a}{48}\Omega,\tag{35}$$

where $K[m']$ is the elliptic integral of the first kind and $\hat{F}(\Omega)$ is defined in Appendix B. In order to calculate T_2, the explicit relations defining the integral functions in Eq. (30) and detailed in Appendix B have been used.

The inner current density J_{in} is determined by solving Eq. (14). J_{in} is then used in Eq. (18) to construct the inner matching function. Algebraic details are given in Appendix

B. As a result of the matching procedure, we find a relation for the saturated island size in the nonrelaxed large island regime:

$$\Delta' = w_s[0.8a^2 - 0.27b - 0.09a]. \tag{36}$$

A significant difference between Eq. (36) and the saturation relation for the small island limit [Eq. (26)] is the absence of the logarithmic term and of the term proportional to A in Eq. (36). We note that this is basically due to the different structure of $\eta = \eta(\Omega)$ in the large island case. Indeed, if the calculation for the large island were extended to take into account the effect of the narrow region around the separatrix, i.e., the thermal boundary layer, we would recover the two missing terms, although multiplied by a factor proportional to the area of the boundary layer where $\eta = \eta(X,\xi) \neq \eta(\Omega)$. Hence, the calculation presented in this section is strictly valid in the limit $w_c/w \rightarrow 0$, while a Padé approximation between Eqs. (36) and (26) might allow for a finite w_c. Further mathematical discussion on this issue and on the origin of the $w \ln w$ and A terms is given in Appendix A.

C. Third scenario: The relaxed large island case

In the third scenario, we concentrate on a longer time scale for the magnetic evolution, such that the perpendicular thermal transport is able to eliminate the steep temperature gradients described in the preceding subsection. This relaxation would initially commence in the thermal boundary layer at the separatrix of the island, but spreads outward and induces a modification of the global equilibrium and, consequently, of the outer linear perturbation. We envisage the following boundary conditions. We assume that plasma edge physics maintains a fixed temperature at $x \rightarrow +\infty$, and that an unchanging heat source in the plasma core maintains a prescribed heat flux; i.e., a constant (dT/dx) at $(x \rightarrow -\infty)$. The new effect, relevant in this case, can then be described by a correction ΔT to the temperature profile obtained for the nonrelaxed case. In order to balance this adjustment of T and to keep the total current constant, as would happen in a tokamak device, we must allow for a change in the value of the external electric field, i.e., $\Delta E = w\Delta E_1 + w^2 \Delta E_2$ (constant in space):

$$\int_0^a r dr E_z T^{3/2} = \int_0^a r dr (E_z + \Delta E)(T + \Delta T)^{3/2}. \tag{37}$$

Using this relation it is, in principle, possible to evaluate ΔE to order $O(w)$ so as to construct a new "quasi-cylindrical" equilibrium and to calculate (numerically) a new value of the tearing index Δ'. The procedure for this calculation is presented in Appendix D, where a specific example is calculated.

It will be useful to expand the correction to the temperature in powers of w, as we already did for T and Ω, $\Delta T = w\Delta T_1 + w^2 \Delta T_2 + \cdots$. Thus, in order to compensate for the jump of the temperature at the edge of the island (i.e., the discontinuity in T in the nonrelaxed large island limit, where the effect of $\kappa_\perp$ is neglected), a constant shift must be applied to T_1:

$$\frac{\Delta T_1}{T_0} = (1 - \sigma H)\tilde{k}\frac{r_s T'_{\mathrm{eq}}(r_s)}{T_0} \equiv \frac{2}{3}\tilde{k} a_s (1 - \sigma H), \tag{38}$$

where $\tilde{k} \approx 0.345$ and $T_0 = T_{\mathrm{eq}}(r_s)$. As a consequence of this change, due to the continuity constraint for $T(\Omega)$ on the separatrix, the equilibrium temperature is also modified far from the reconnecting surface (see Fig. 1). The equilibrium current density consistent with the new temperature profile is characterized, up to the order of interest, by different values of $J_{\mathrm{eq}}(r_s)$, $J'_{\mathrm{eq}}(r_s)$, $J''_{\mathrm{eq}}(r_s)$, and $s(r_s)$ for $X<0$ and $X>0$. For positive values of X, the equilibrium parameters a_s and b_s, are unchanged [indeed, $J^{+}_{\mathrm{eq}}(0)/\rho = J_{\mathrm{eq}}(0)$, $J'^{+}_{\mathrm{eq}}(0)/\rho = J'_{\mathrm{eq}}(0)$, $J''^{+}_{\mathrm{eq}}(0)/\rho = J''_{\mathrm{eq}}(0)$, with $\rho = (E + \Delta E)/E$], while $s^{+}(0) = s(0) + (\Delta E/E)[s(0) - 2]$, so that one obtains

$$a^{+} = a\left(1 + \frac{2}{s}\frac{\Delta E}{E}\right), \tag{39}$$

$$b^{+} \cong b, \tag{40}$$

where the corrections to the parameter b have been dropped since they give a higher-order modification to our calculation. For negative X (the calculation is given in Appendix D):

$$a^{-} = a\left[1 + \frac{2}{s}\frac{\Delta E}{E} + \frac{2\Delta T}{T}\left(1 - \frac{3}{s}\right)\right], \tag{41}$$

$$b^{-} \cong b, \tag{42}$$

where, again, only the relevant order of b is kept. Consequently, the difference, $a^{+} - a^{-} = w(4/3)\tilde{k} a a_s (1 - 3/s)$. Equation (9) for the perturbed magnetic flux must be solved separately on the two sides of the resonant layer, in order to take into account the new features of the equilibrium current density. In the left branch of the linear solution, described in expression (10), a is then replaced by a^{-}. In addition, the asymmetry of the magnetic flux within the nonlinear region implies that also the arbitrary constant ψ_{*0} is no longer the same for the two (i.e., left and right) eigenfunctions. If we set $\psi^{+}_{*0} = \psi_{*0}$ for $\tilde{\psi}^{+}_{\mathrm{out}*}$, then $\psi^{-}_{*0} = \psi_{*0} + w^3 \Delta\psi$ for $\tilde{\psi}^{-}_{\mathrm{out}*}$, where $\Delta\psi = O(1)$ can be determined by an unusual inverse matching procedure with a suitable solution of the modified flux function in the inner region (see below). Note that $w^3 \Delta\psi$ is a relevant $O(w)$ correction to ψ_{*0}, since $\psi_{*0} = O(w^2)$.

Indeed, ΔT modifies the current density through Eq. (19) and yields a correction of the magnetic flux at each order in w. From the new Ampère's law, we then obtain

$$\frac{\partial^2 \Omega_1}{\partial X^2} = 16a\frac{T_1}{T'_{\mathrm{eq}}(r_s)} - \frac{1}{r_s}\frac{\partial \Omega_0}{\partial X} + 16a\frac{\Delta T_1}{T'_{\mathrm{eq}}(r_s)} + 16\frac{\Delta E_1}{E_z}\left(1 - \frac{2}{s}\right). \tag{43}$$

The comparison of this equation with Eq. (32) shows that the variation of the magnetic flux with respect to the nonrelaxed large island case is

$$\Delta\Omega_1 = (1-\sigma H)(8X^2\tilde{k}a + 8X_m^2\tilde{k}a) - (1-H)16X_m X\tilde{k}a + 8\frac{\Delta E_1}{E_z}\left(1-\frac{2}{s}\right)X^2, \quad (44)$$

where $X_m=\sqrt{1+\cos\xi}/\sqrt{8}$ and the constants of integration have been chosen to assure continuity of $\Delta\Omega_1$ and of its first derivative on the separatrix. It should be noted that in the region to the left of the island ($\sigma=-1$), the term proportional to X_m^2 gives a negligible, i.e., $O(w^3)$, contribution to the equilibrium and a relevant, i.e., $O(w)$, correction to the perturbation. Indeed, it is the term proportional to $\cos\xi$ in X_m^2 that induces the asymmetry of the inner solution and causes the $\Delta\psi$ shift in the outer region. This can now be completely determined through the inverse matching procedure, yielding $\Delta\psi=-\tilde{k}aJ_{\mathrm{eq}}(0)/8$.

This relevant modification of the outer solution represents a significant departure with respect to the small island case and to the nonrelaxed large island case. An important consequence is that extra terms appear in the outer matching function, which are absent in Eq. (11), as can easily be seen by substituting the new $\tilde{\psi}^+_{\mathrm{out}*}$ and $\tilde{\psi}^-_{\mathrm{out}*}$ in the definition (12):

$$M_{out}^{\mathrm{NRLI}}(X) = M_{\mathrm{out}}(X) + w\left[\left(4a^2 - \frac{2}{3}aa_s\right)\tilde{k}(\ln|X| + \ln w + 1) + Aa\tilde{k}\right]. \quad (45)$$

The introduction of a change in the magnetic flux $\Delta\Omega_1$ implies a variation of the magnetic island shape and, consequently, of the averaging operators defined in Eq. (13), which are related to $\Delta\Omega_1$ through the metric term $\partial_X\Omega$. This entails a self-consistent correction of the temperature to order w^2, ΔT_2, [cf. the term $\partial_X\Omega|_1$ in Eq. (30)]:

$$\frac{d\Delta T_2}{d\Omega} = -\frac{\sigma 2\pi T'_{\mathrm{eq}}(r_s)\int_0^{2\pi} d\xi\left(\frac{\partial\Delta\Omega_1}{\partial X} - \frac{\Delta\Omega_1}{X}\right)}{\left(\int_0^{2\pi} d\xi\ \left.\frac{\partial\Omega}{\partial X}\right|_0\right)^2}. \quad (46)$$

It should be noted that T_2, different from the nonrelaxed large island case, does not have a definite parity. For the purpose of the present paper, we need to evaluate only the even part of the correction, since, as shown in Appendix C, the odd part does not enter the calculation of the matching function. Thus, by integrating the equation above, we obtain

$$\Delta T_{2\mathrm{EVEN}} = \frac{H\pi\sqrt{2}\tilde{k}aT'_{\mathrm{eq}}(0)}{32}\int_\Omega^\infty\left[\frac{K(1-\Omega')}{E^2(\Omega'+1)^{3/2}} + \frac{2}{\pi\sqrt{\Omega'}}\right] + \frac{H\sqrt{2}}{8}\tilde{k}aT'_{\mathrm{eq}}(0)\sqrt{\Omega}. \quad (47)$$

Finally, knowing ΔT_2, we can find J_{RLI} up to the order of interest. Similar to the cases treated earlier, the knowledge of the inner current density allows the evaluation of M_{in}. Matching onto the outer solution, as described in Appendix C, yields the saturation relation for the relaxed large island limit:

$$\Delta' = w_s\left\{a^2\left[1.39\ln\left(\frac{1}{w_s}\right)+1\right] + aa_s\left[-0.23\ln\left(\frac{1}{w_s}\right)+0.07\right] - 0.27b - 0.69a - 0.347Aa\right\}. \quad (48)$$

We emphasize the presence in the expression above of a logarithmic term. Nevertheless, the origin of this term is substantially different from its counterpart in Eq. (26). Indeed, its occurrence is due to the imbalance between the two branches of the perturbed outer magnetic flux solution that generates ΔM_{out}, so it is not related to the inner current structure as in the small island case. The scale invariance of the logarithmic term in Eq. (48) is assured by the combination with Δ' which is calculated using the new relaxed equilibrium. We remark that indeed, the change of the equilibrium parameters after the relaxation implies the scale dependence of the Δ' term alone.

VI. SLAB GEOMETRY

In this section, we present the equivalent of the saturation relations (26), (36), and (48) for slab geometry. In this case, the outer magnetic flux solution is simplified. Equation (9) now becomes

$$\frac{\partial^2\tilde{\psi}_*}{\partial x^2} - \left(k^2 + b_s - \frac{a_s^2}{2} + \frac{a_s}{x}\right)\tilde{\psi}_* = 0. \quad (49)$$

In Eq. (49), k is the mode wave vector along the "poloidal" direction: $y=r_s\xi$. Consequently, the asymptotic behavior of the magnetic flux and the matching function change into

$$M_{\mathrm{out}}(X) = \Delta' + w\left\{2a_s^2X\ln|X| + 2X\times\left[\left(\frac{Aa_s}{2} + a_s^2\ln w\right) + k^2 + b_s - \frac{3}{2}a_s^2\right]\right\} + O(w^2\ln w). \quad (50)$$

Furthermore, we remark that, in contrast to the cylindrical case, in slab geometry the helical current density, i.e., $J_*=-\nabla_\perp^2\Psi_*$, coincides with the current density J along the z direction. Since the Laplacian operator is now simply: $\nabla_\perp^2=\partial_x^2+\partial_y^2$, first derivatives of ψ_* do not appear in the integral defining M_{in}. For the same reason, the perturbative expansion of Ampère's law, which gives the island structure in the singular layer, is also modified. Indeed, although Eqs. (22) and (31) are not modified, Eq. (23) is replaced by

$$\frac{\partial^2\Omega_1}{\partial X^2} = 16a_s\langle X\rangle_0, \quad (51)$$

and Eq. (32) by

$$\frac{\partial^2\Omega_1}{\partial X^2} = 16a_s\frac{T_1}{T'_{\mathrm{eq}}(r_s)}, \quad (52)$$

where in both expressions we have used the identity $16J_*/J_{*\mathrm{eq}}=16J/J_{\mathrm{eq}}$. Hence, in Ω_1, the term proportional to

X^3 disappears and all the terms involving a become proportional to a_s instead.

Similarly, in the small island calculation, the functions P and Q (see Appendix A) undergo similar modifications, which lead to the disappearance of the terms proportional to a and $1/(2-s)$ in the final saturation relation. Thus, the slab result in the small island limit becomes

$$\Delta' = 0.41 w_{s\mathrm{SLAB}} \left\{ a_s^2 \left[\ln\left(\frac{1}{w_{s\mathrm{SLAB}}}\right) + 4.85 \right] - \frac{A a_s}{2} - b_s \right\}. \tag{53}$$

In the nonrelaxed large island case (second scenario), the changes to the temperature profile due to the new geometry are effective only in order w^2. Indeed, Eqs. (28) and (29) are unaltered, while the new shape of Ω_1 affects the integral function (B6) in Eq. (30), so that a_s^2 replaces a^2 and the term proportional to a disappears. Furthermore, we observe that in the case treated here, the correct relation between the temperature and the perpendicular conductivity is $\kappa'(r_s)/\kappa(r_s) = -T''_{\mathrm{eq}}(r_s)/T'_{\mathrm{eq}}(r_s)$; i.e., the only way to take into account consistently the second derivative of T_{eq} is to allow for a finite radial gradient of $\kappa_\perp$. As a result, in slab geometry Eq. (35) is replaced by

$$\Delta' = w_{s\mathrm{SLAB}}[0.8 a_s^2 - 0.27 b_s]. \tag{54}$$

Finally, in the relaxed large island case (third scenario), we observe that the calculations of $\Delta\Omega_1$, ΔT_1, and ΔT_2 are not affected by geometrical considerations. This implies that the saturation relation undergoes the same modification as in Eq. (54), so that, for the relaxed large island case, we obtain

$$\Delta' = w_{s\mathrm{SLAB}} \left\{ a_s^2 \left[1.16 \ln\left(\frac{1}{w_{s\mathrm{SLAB}}}\right) + 1.07 \right] - 0.27 b_s - 0.34 A a_s \right\}. \tag{55}$$

VII. CONCLUSIONS

The saturation of the tearing mode in a plasma column has been investigated in three different physical regimes. The cylindrical geometry and the physical models that we have employed are quite well suited to represent the growth of a magnetic island in a region far from the core and from the scrape-off layer of a confined plasma for magnetic fusion. The starting point of our mathematical analysis has been the perturbative procedure and the asymptotic matching method introduced by Thyagaraja.[12] These techniques have been extended and complemented in order to derive a fully nonlinear and self-consistent solution to the tearing mode saturation problem in the three cases treated. The investigation presented has achieved two interesting results.

First, we have significantly extended previous theoretical analysis on the saturation of the tearing mode in the small island case; i.e., when the temperature and resistivity profiles are unaffected by the presence of the magnetic field perturbation. In particular, the saturated island width given by relation (26) is appreciably different from the predictions of previous calculations, as shown in Fig. 3. We note, as an

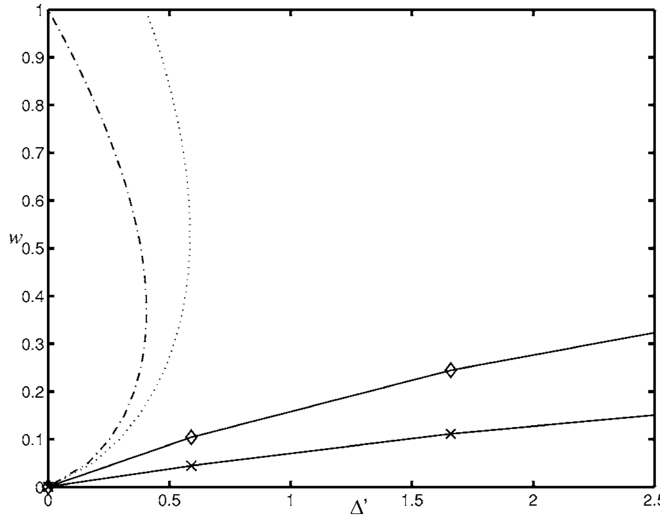

FIG. 3. Comparison between the saturation relations for a typical bell shaped current density profile. The dot-dashed line is Thyagaraja's dispersion relation with the normalizing length scale $L=1$. The dotted line is Pletzer and Perkins relation. The small island [Eq. (26)] and the nonrelaxed large island [Eq. (36)], relations are represented by the cross and diamond solid lines, respectively.

example, that our solution does not imply the occurrence of a tangent bifurcation for w_s in the range of validity of the model, as distinct from Refs. 12–14. Indeed, the logarithmic term, responsible for the tangent bifurcation, in Eq. (26) is dominant only for very small island (or so large that the $w \ll 1$ approximation fails). Furthermore, the perturbative technique that we have employed allowed us to evaluate the magnetic island shape in a self-consistent way, while the calculations in Refs. 7, 13, and 14 relied on an ansatz.

The second main result is relevant to larger islands ($w \gg w_c$), such that the effect of the modification of η becomes relevant. In this regard, we have introduced an energy equation that controls the thermal transport in the island region, and we have solved it self-consistently with the modified magnetic structure. In the integration of Eq. (17) two alternative sets of boundary conditions have been used, corresponding to different physical states. In the first case—the nonrelaxed large island regime—we have assumed that the saturation of the magnetic field perturbation occurs faster than the time scale for the perpendicular thermal transport. That might be the case, for example, for magnetic islands driven by a sawtooth event in a tokamak. Since the global thermal equilibrium is not modified by the change in the magnetic field, we then assume that the perturbed temperature matches the original equilibrium temperature far from the reconnecting surface.

However, this solution represents a temporary equilibrium state, since it is not in thermal equilibrium and after the saturation of the island the steep temperature gradient at the separatrix will relax as a consequence of the perpendicular thermal transport, which leads to the relaxed large island state. Hence, the relaxed large island regime, has a more general validity because it can also fit the behavior of a tearing mode that has evolved on a slower resistive time scale,[2] which is typically longer then the cross-field thermal diffusion time $\tau_{\kappa_\perp}$. An important outcome of our solution is that, although the temperature perturbation is generated locally by the presence of the island, it spreads outward and significantly modifies the equilibrium in the linear region.

We emphasize that, for the same equilibrium parameters, the large island saturated widths obtained from Eqs. (36) and the widths calculated using relation (26) are considerably different (see Fig. 3), which necessarily implies that the models based on the assumption of an unperturbed resistivity cannot give an adequate description of the saturation of the island when $w \gg w_c$.

The main limitations of the present calculation are the neglect of diamagnetic, ion Larmor radius (ρ_i) and three-dimensional effects. The first two effects are known to influence the island behavior only when its width is small, namely, when $w \lesssim \rho_i$, while the three-dimensional effect plays a role in the opposite limit, when the width of islands located on different resonant surfaces (i.e., with different helicities) is so large that they overlap. On the other hand, the presented nonlinear calculation provides a theoretical framework open to extensions to more complex physics.

Another limitation comes from having neglected pressure effects. Apart from neoclassical bootstrap effects, pressure corrections modify the saturated island relation, as shown in Refs. 19–21, into $\Delta' = a^* w_s - \alpha^* \beta / w_s$, where a^* is the factor multiplying w_s, e.g., in Eq. (48), and α^* is a numerical factor of order unity (for standard values of the magnetic shear parameter and of the equilibrium pressure length). Thus, we can see that although pressure effects may be very important for small islands, they will be insignificant at saturation provided that beta is small enough; i.e., $\beta \ll (1/a^*)\Delta'^2$.

An interesting application of the nonlinear procedure could be the investigation of force free configurations, such as those typical of the reversed field pinches (RFPs). Here, the evolution and saturation of a magnetic island, due to a tearing instability, might provide a viable mechanism for the transition to the quasi-single-helicity configurations observed in experiments and numerical simulations. Furthermore, Arcis *et al.*[22] have pointed out that the nonlinear modification of the outer magnetic flux function ψ_{out}, discussed in Ref. 15 and here in Sec. V [see discussion after Eq. (27)], together with flux conserving boundary conditions at the plasma wall, may be responsible for field reversal in an RFP as a magnetic island develops and saturates starting from a paramagnetic pinch equilibrium. We stress that the formulae (26), (36), and (48) for the saturated island width, derived in this paper, are not directly applicable to RFP plasmas, but the method established in this paper can be adopted to obtain the equivalent results for the RFP case.

The new resistive MHD terms we have derived, appearing in the island saturation relations, can be expected to have some impact on neoclassical tearing modes (NTMs). Indeed, the three saturation relations [Eqs. (26), (36), and (48)] can be written as $\Delta' = \alpha w$, with α nearly a constant [α contains a term proportional to $\ln w$ in Eqs. (26) and (48)]. The parameter α, viewed as a function of the resonant radius r_s is large and positive for a typical current density profile in a tokamak. For instance, focusing on the small island case, assuming the peaked current density profile, i.e., $J = J_0(1-r^2)^2$ (with $r=1$ the plasma edge), and taking, for simplicity, $\ln(1/W)=4$, we find $10 < \alpha(r_s) < 55$ for the $m/n=2/1$ tearing mode, as the location of the resonant surface r_s is varied. The higher values of α are attained near the plasma center. For this current density profile, the $2/1$ mode is unstable (with conducting wall boundary conditions) when $r_s \leq 0.88$, at which point $\alpha \simeq 16$. Thus, since α is so large, we can expect that the new resistive MHD terms we have derived will have some impact on the saturation level of NTMs.

Finally, we note that the method and framework established in the calculation of the large saturated islands (scenarios 2 and 3) could be extended to investigate the effect of a localized heat source (or current drive) such as electron cyclotron resonance heating (ECRH) routinely provides in many tokamak devices. For ECRH localized around the median plane in a tokamak this might be realistically modeled with a local heat source of the form $Q = Q_0 \exp[-\alpha(X-X_0)^2]$ in the electron thermal equation for T.

ACKNOWLEDGMENTS

The authors are happy to acknowledge fruitful discussions with N. Arcis, D. Escande, M. Ottaviani, and A. Smolyakov.

APPENDIX A: SMALL ISLAND MATCHING

The purpose of this appendix is to give some mathematical details of the calculation in the small island limit. We begin by deriving the normalized magnetic flux to order w. This is obtained by integrating Eq. (23) by parts:

$$\langle X \rangle = \frac{\displaystyle\int_0^\alpha \frac{d\xi X}{|\partial_X \Omega|}}{\displaystyle\int_0^\alpha \frac{d\xi}{|\partial_X \Omega|}} = \frac{\displaystyle\int_0^\alpha \frac{d\xi X}{|16X + wP|}}{\displaystyle\int_0^\alpha \frac{d\xi}{|16X_0 + wQ|}} = \frac{\sigma \displaystyle\int_0^\alpha \frac{d\xi}{16} - w \int_0^\alpha \frac{P}{16^2|X_0|}}{\displaystyle\int_0^\alpha \frac{d\xi}{16|X_0|} - w\sigma \int_0^\alpha \frac{Q}{16^2 X_0^2}},$$

where $P = \partial_X \Omega_1$, $Q = \partial_X \Omega_1 - \Omega_1 / X$ and $X_0 = \sigma\sqrt{\Omega + \cos\xi}/\sqrt{8}$ is the zeroth-order term of the expansion of X as a function of the magnetic variables Ω and ξ. Thus, we have

$$\langle X \rangle_0 = \sigma H \frac{\sqrt{2}\pi}{2} \frac{1}{\displaystyle\int_0^\alpha \frac{d\xi}{\sqrt{\Omega + \cos\xi}}}, \tag{A1}$$

$$\langle X\rangle_1 = -\frac{1}{16}\frac{\int_0^\alpha \frac{d\xi P}{\sqrt{\Omega+\cos\xi}}}{\int_0^\alpha \frac{d\xi}{\sqrt{\Omega+\cos\xi}}} + \frac{\pi}{8}\frac{\int_0^\alpha \frac{d\xi Q}{\Omega+\cos\xi}}{\left(\int_0^\alpha \frac{d\xi}{\sqrt{\Omega+\cos\xi}}\right)^2}, \tag{A2}$$

where $\sigma=|X|/X$, $H=H(\Omega-1)$ is the Heaviside function (so that $\langle X\rangle_0=0$ inside the island), and $\int_0^\alpha d\xi/\sqrt{\Omega+\cos\xi}$ can be expressed in terms of elliptic integrals, as shown, for example, in Ref. 23. We also note that the $O(w)$ part of the average $\langle X\rangle_1$ will be used to calculate J_{SI2} in Eq. (16).

Hence, Eq. (23) can be written as

$$\frac{\partial^2\Omega_1}{\partial X^2} = \frac{4\pi\sigma a H}{\sqrt{m}K(m)} - 16X, \tag{A3}$$

where K is the elliptic integral of the first kind and $m=2/(\Omega+1)$. The integration of this equation must be carried out separately in the three regions, $-1<\Omega<1$ (i.e., inside the island), and $\Omega>1$, $\sigma\pm1$ (i.e., outside the island separatrix, on the right and on the left). This introduces six arbitrary functions, i.e., $C_j(\xi)$, $(j=1,6)$, which are then determined by applying appropriate boundary conditions. These are continuities of Ω_1 and $\partial\Omega_1/\partial X$ on both the left separatrix $(\Omega_0=1,\sigma=-1)$ and the right separatrix $(\Omega_0=1,\sigma=+1)$ and matching Ω_1 to the outer region solution for $|X|\to\infty$. The result of this procedure yields Eq. (25), where the functions G_1 and $G_2$are defined as

$$G_1(\Omega,\xi) = \frac{\pi}{2}H\int_1^\Omega d\Omega'\left[\frac{\dfrac{\sqrt{\Omega'+1}}{K\left(\dfrac{2}{\Omega'+1}\right)} - \dfrac{2}{\pi}\sqrt{\Omega'}}{\sqrt{\Omega'+\cos\xi}}\right] - \frac{\pi}{2}\int_1^\infty d\Omega'\left[\frac{\dfrac{\sqrt{\Omega'+1}}{K\left(\dfrac{2}{\Omega'+1}\right)} - \dfrac{2}{\pi}\sqrt{\Omega'}}{\sqrt{\Omega'+\cos\xi}}\right], \tag{A4}$$

$$G_2(\Omega) = -\frac{\sqrt{2}}{6} + \frac{\sqrt{2}\pi}{8}\int_1^\Omega d\Omega'\left[\frac{\sqrt{\Omega'+1}}{K\left(\dfrac{2}{\Omega'+1}\right)} - \frac{2}{\pi}\sqrt{\Omega'}\right]. \tag{A5}$$

Having constructed the flux function $\Omega=\Omega_0+w\Omega_1$, correct to order $O(w)$, it is now possible to return to the expression for $\langle X\rangle$ and, knowing P and Q, to construct $\langle X\rangle$ correct to $O(w)$, which is required for the evaluation of J_{SI2}. In this regard, it is useful to display the structure of Q:

$$Q = \frac{2}{3}aH\left[\frac{\Omega^{3/2}+3\sqrt{2}G_2(\Omega)}{\sqrt{\Omega+\cos\xi}}\right] - \frac{2}{3}\Omega + \cos\xi, \tag{A6}$$

where, the identity $X(\partial_X G_1)=\sigma\partial_X G_2$ has been used. Now, with the current density known up to order w^2, we can substitute it in the definition of the matching function $M_{in}(X)$: Eq. (15).

In order to calculate the integral in Eq. (15) and noting that the current density is a function of Ω only, it would be natural to switch to a magnetic flux coordinate as integration variable: $(X,\xi)\to(\Omega,\xi)$. However, this gives rise to some technical difficulties, which are related to the fact that the region of integration of Eq. (15) is symmetric with respect to the radial coordinate X, while Ω is not. For this reason, the integration in Ω must be taken to slightly different limits on the two sides $\sigma=\pm1$. As an alternative one can, instead of using the total normalized flux function, use the coordinate Ω_0, which has the required symmetry properties. It is then necessary to express J_{SI} as a function of this new coordinate and of the helical variable ξ:

$$J_{SI}(\Omega) = J_{SI}(\Omega_0 + w\Omega_1 + \cdots) = J_{SI}(\Omega_0) + wJ'_{SI}(\Omega_0)\Omega_1 + \cdots, \tag{A7}$$

where the prime indicates a derivative with respect to Ω. However, if Ω_0 is used as the integration variable, extra care is required in defining the interior of the island, since the separatrix, is defined by $\Omega=1$, not by $\Omega_0=1$. In practice, both methods were used in the evaluation of M_{in}.

It should be noted that the calculation of M_{in} is quite delicate, since the dominant part of the integral, which gives rise to divergencies, must be separated from the rest. The divergencies thus obtained match automatically onto their counterparts in M_{out}, while Eq. (26) corresponds to the numerical integration of the convergent part. Furthermore, the integral of the term due to the cylindrical approximation in Eq. (15) (i.e., the second term inside the bracket) can be calculated noting that

$$-\frac{1}{\pi\psi_{*0}}\int_{-X}^{X} dX\int_0^{2\pi} d\xi\cos\xi\left[(1-wX)\frac{\partial\Psi_*}{\partial X}\right] = \frac{w}{\pi}\int_0^{2\pi} d\xi\cos\xi\,\Omega_1\Big|_{-X}^{X}, \tag{A8}$$

which gives only a divergent part.

Finally, we want to stress that the $w\ln w$ and A terms in the small island saturation relation are linked to the average of X and, in particular, to the quantity P. We draw the attention to the fact that, for every model which allows for an explicit X dependence for the resistivity in some region of the plasma, it is possible to Taylor expand η, thus introducing an $\langle X\rangle$ term in the expression for the current density; hence, $w\ln w$ and A terms in the saturation relation will appear. This situation occurs, for example, in presence of a narrow thermal boundary layer in the vicinity of the separatrix, which is produced by a finite $\kappa_\perp$ in the large island models.[3] However, in the nonrelaxed large island case, these terms are multiplied by a factor $O(w_c/w)\ll1$, and therefore can be neglected.

APPENDIX B: NONRELAXED LARGE ISLAND: MATHEMATICAL DETAILS

In this appendix, details of the nonrelaxed large island calculation and of the matching procedure are given. First, we focus on the system of Eqs. (28)–(30). It is possible to express the integral function in Eq. (29) in terms of an elliptic integral of the second kind (E):

$$\int_0^{2\pi} d\xi 4\sqrt{2}\sqrt{\Omega+\cos\xi} = 32\frac{E(m)}{\sqrt{m}}l, \tag{B1}$$

where $m=2/(\Omega+1)$.

Using this result, it is straightforward to integrate Eq. (29) and to obtain Eq. (33), where it has been imposed that the asymptotic behavior of T_1 matches onto the outer linear solution. The magnetic flux to order w is then found upon integrating Eq. (32) by parts, which gives Eq. (34), with

$$F_1(\Omega,\xi) = \frac{\pi}{2}H\int_1^{\Omega} d\Omega'\left[\frac{\hat{F}(\Omega')}{\sqrt{\Omega'+\cos\xi}}\right] - \frac{\pi}{2}\int_1^{\infty} d\Omega'\left[\frac{\hat{F}(\Omega')}{\sqrt{\Omega'+\cos\xi}}\right], \tag{B2}$$

$$F_2(\Omega) = -\frac{\sqrt{2}}{6} + \frac{\sqrt{2}\pi}{8}\int_1^{\Omega} d\Omega'\hat{F}(\Omega'), \tag{B3}$$

and

$$\hat{F}(\Omega) = -\int_{\Omega}^{\infty} d\Omega'\left[\frac{1}{2\sqrt{\Omega'+1}E\left(\frac{2}{\Omega'+1}\right)} - \frac{1}{\pi\sqrt{\Omega'}}\right]. \tag{B4}$$

Now, we evaluate the integral function in Eq. (30):

$$\int_0^{2\pi} d\xi X \left.\frac{\partial\Omega}{\partial X}\right|_0 = \int_0^{2\pi} d\xi 2(\Omega+\cos\xi) = 4\pi\Omega, \tag{B5}$$

$$\int_0^{2\pi} d\xi \left.\frac{\partial\Omega}{\partial X}\right|_1 = \sigma\int_0^{2\pi} d\xi\left\{\frac{a}{X}\left[\frac{\sqrt{2}}{6}\Omega^{3/2}+F_2(\Omega)\right] - \frac{16}{3}X^2\right\}, \tag{B6}$$

$$= \sigma a\left[\frac{\sqrt{2}}{6}\Omega^{3/2}+F_2(\Omega)\right]\frac{8\sqrt{2}K\left(\frac{2}{\Omega+1}\right)}{\sqrt{\Omega+1}} - \sigma\frac{4\pi}{3}\frac{\Omega}{r_s}. \tag{B7}$$

The integration of Eq. (30) yields Eq. (35) and hence the current density up to order w^2.

Equation (15) is completely determined, so it can be substituted in the inner matching function Eq. (18). It is easily seen that M_{in} becomes

$$M_{\mathrm{in}}(X) = 2wk^2X - \frac{w}{\pi}\left(1-\frac{2}{s}\right)\int_{-X}^{X} dX'\int_0^{2\pi} d\xi\cos\xi \times\left[24\frac{T_2}{T_0}+6\left(\frac{T_1}{T_0}\right)^2\right]. \tag{B8}$$

Note that the integration of the $O(1)$ and $O(w)$ parts of J_{LI} give no contribution to the above relation, because the first is constant, while the second is odd in X. As in the small island case, also the integral of the metric term due to the cylindrical geometry in Eq. (11) gives only a divergent part.

Finally, we can calculate the double integral in Eq. (B8) using Ω_0 instead of the radius as integration variable. After expanding T_1 and T_2 in terms of the new variables [i.e., $T(\Omega)=T(\Omega_0)+wT'(\Omega_0)\Omega_1+\cdots$], it is possible to separate the dominant part of the integral (that matches automatically with the divergencies in M_{out}) from the subdominant part. This leads to the saturation relation (36), where the numerical factors result from numerical integration.

APPENDIX C: RELAXED LARGE ISLAND: MATHEMATICAL DETAILS

The mathematical treatment of the relaxed large island case relies on the introduction of a correction to the nonrelaxed large island model. For this reason, the calculation of the new normalized flux function is somewhat simpler than in the other two cases. Indeed, the main body of Ω_1 has already been evaluated in Appendix B, while the correction is given by the calculation in this appendix.

Nevertheless, the presence of a term that induces a relevant modification to the outer magnetic flux and the loss of the parity of Ω_1 are nontrivial issues. The latter also entails the loss of parity of the corrected metric term $\partial_X\Omega|_1$, so that

$$\left.\frac{\partial\Delta\Omega}{\partial X}\right|_1 = 8\frac{\Delta E}{E_z}X + 8\tilde{k}aX - \frac{8\tilde{k}aX_m^2}{X} - \sigma\left(8aX\tilde{k}+\frac{8\tilde{k}aX_m^2}{X}\right), \tag{C1}$$

where the last two terms in the expression are even functions with respect to X. Consequently, now ΔT_2 also shows a mixed parity. We remark that the integrals in Eq. (46) can be expressed as a combination of elliptic integral functions. Once ΔT_2 is calculated self-consistently, it is used to obtain the corrected inner matching function. Hence,

$$M_{in}(X) = 2wk^2X - \frac{w}{\pi}\left(1-\frac{2}{s}\right)\int_{-X}^{X} dX'\int_0^{2\pi} d\xi\cos\xi\left\{\left[24\frac{T_{2\mathrm{NRLI}}}{T_{0\mathrm{NRLI}}}+6\left(\frac{T_{1\mathrm{NRLI}}}{T_{0\mathrm{NRLI}}}\right)^2\right] + \left[24\frac{\Delta T_{2\mathrm{EVEN}}}{T_{0\mathrm{NRLI}}}+6\left(\frac{\Delta T_1}{T_{0\mathrm{NRLI}}}\right)^2+12\frac{T_{1\mathrm{NRLI}}\Delta T_{1\mathrm{ODD}}}{T_{0\mathrm{NRLI}}^2}\right] + \frac{w}{\pi}\int_0^{2\pi} d\xi\cos\xi\Omega_1|_{-X}^{X}, \tag{C2}$$

where the subscript "NRLI" indicates the temperature in the nonrelaxed model, given by Eqs. (33) and (34). Note that in Eq.

(C2) only the even part of T_2 is needed, since the odd part gives no contribution to the integral. Similarly, the odd parity of $T_{1\mathrm{NRLI}}$ requires the odd part of ΔT_1 in Eq. (C2).

Most of the terms of M_{in} have already been calculated in Appendix B, as clearly seen by comparing Eq. (C2) with Eq. (B8). The residual part, i.e., the integral of the last three terms of the integrand, is calculated by replacing the radial integration variable with the symmetric magnetic variable Ω_0, so that

$$M_{\mathrm{in}} = M_{\mathrm{in\ NR}}(X) - \frac{\sqrt{2}w}{4\pi}\left(1-\frac{2}{s}\right)\int_1^{\Omega_0} d\Omega_0' \int_0^{2\pi} d\xi \frac{\cos\xi}{\sqrt{\Omega_0'+\cos\xi}} \times\left[24\frac{\Delta T_{2\mathrm{EVEN}}}{T_{0\mathrm{NR}}} + 6\left(\frac{\Delta T_1}{T_{0\mathrm{NR}}}\right)^2 + 12\frac{T_{1\mathrm{NR}}\Delta T_{1\mathrm{ODD}}}{T_{0\mathrm{NR}}^2} + 24\frac{dT_1}{d\Omega}\Delta\Omega_{1\mathrm{ODD}}\right] + \frac{w}{\pi}\int_0^{2\pi} d\xi \cos\xi \Delta\Omega_1 t\big|_{-X}^{X}, \tag{C3}$$

where all the terms in the integral are considered as a function of Ω_0 and ξ. As a result of that and of the change in the normalized flux function, in the previous equation a term proportional to the derivative of T_1 now appears [cf. Eq. (B8) and the discussion at the end of Appendix B]. We remark that the expression above becomes a function of X only far from the reconnecting surface; i.e., in the limit $\Omega_0 \to \infty$. Finally, note that

$$\frac{w}{\pi}\int_0^{2\pi} d\xi \cos\xi \Delta\Omega_1\big|_{-X}^{X} = 2w\tilde{k}a. \tag{C4}$$

In this case as well, the dominant part of the integral gives diverging terms, which are automatically matched in the outer region, while the subdominant convergent part can be evaluated numerically to give the corrections to the saturation relation displayed in Eq. (48).

APPENDIX D: MODIFIED EQUILIBRIUM FOR THE RELAXED LARGE ISLAND CASE

In this appendix, we describe the construction of the modified equilibrium which develops in the presence of a thermally relaxed magnetic island (third scenario of the text) and outline the calculation of Δ' and A as functions of the island width w. An example is calculated explicitly for a specific, typical, initial equilibrium. As described in the main text, under conditions of stably maintained edge temperature and a heat source localized in the plasma core, the effect of a magnetic island in thermal equilibrium with the surrounding plasma is to decrease the core electron temperature, while leaving the temperature in the outer region (i.e., $r > r_s$) unchanged. In a tokamak, the resulting decrease in core current density is compensated for by an increase in the applied loop voltage so that the total plasma current is maintained. The result is a modified current density profile $J_f(r)$, and safety factor profile $q_f(r)$, where we use the subscript "f" to distinguish this final equilibrium from the initial equilibrium in which $J=J(r)$ and $q=q(r)$. Thus, the current profile is given by

$$J_f(r) = \left[1 + \frac{\Delta E}{E} - \frac{3\Delta T}{T(r)}\right]J(r), \quad 0 < r < r_s, \tag{D1}$$

$$J_f(r) = \left(1 + \frac{\Delta E}{E}\right)J(r), \quad r_s < r < 1, \tag{D2}$$

where $\Delta T = 0.23awT(r_s)$ is the temperature drop within the island and ΔE is the increase in the applied electric field. From Ohm's law, assuming Spitzer resistivity and the constant current condition, this electric field can be evaluated as

$$\frac{\Delta E}{E} = \frac{0.69aw}{I}\int_0^{r_s} r\{J(r)J(r_s)^2\}^{1/3} dr, \tag{D3}$$

where $I = \int rJ(r)dr$ is the total toroidal current. In the new equilibrium defined by Eqs. (D1) and (D2) the current gradient is discontinuous at the resonant radius (which has itself moved by a small $O(w)$ distance from its original location). Consequently, the parameters a and b are also discontinuous at r_s, and we must use the generalized definitions of Δ' and A in terms of the coefficients of the large and small asymptotic solutions in the vicinity of r_s. Thus,

$$\Delta' = \lim\left[\frac{r\psi_+'}{\psi_+} - \frac{r\psi_-'}{\psi_-} - (a_+ - a_-)\ln|(r-r_s)/r_s|\right], \tag{D4}$$

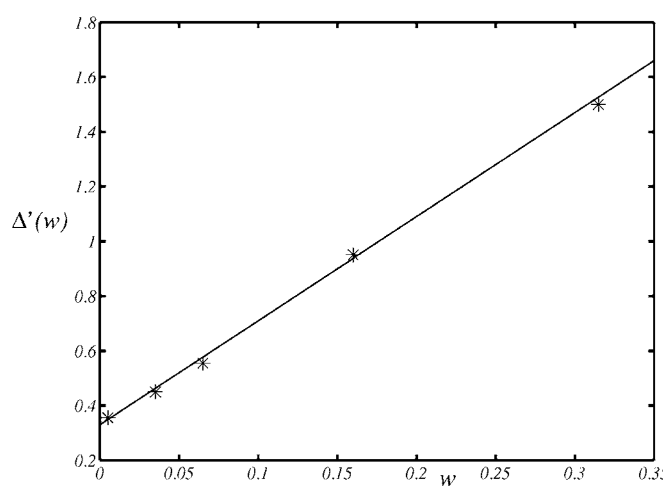

FIG. 4. Numerical results for the linear stability parameter in the new equilibrium (stars). The solid line interpolates the data and is represented by Eq. (D6).

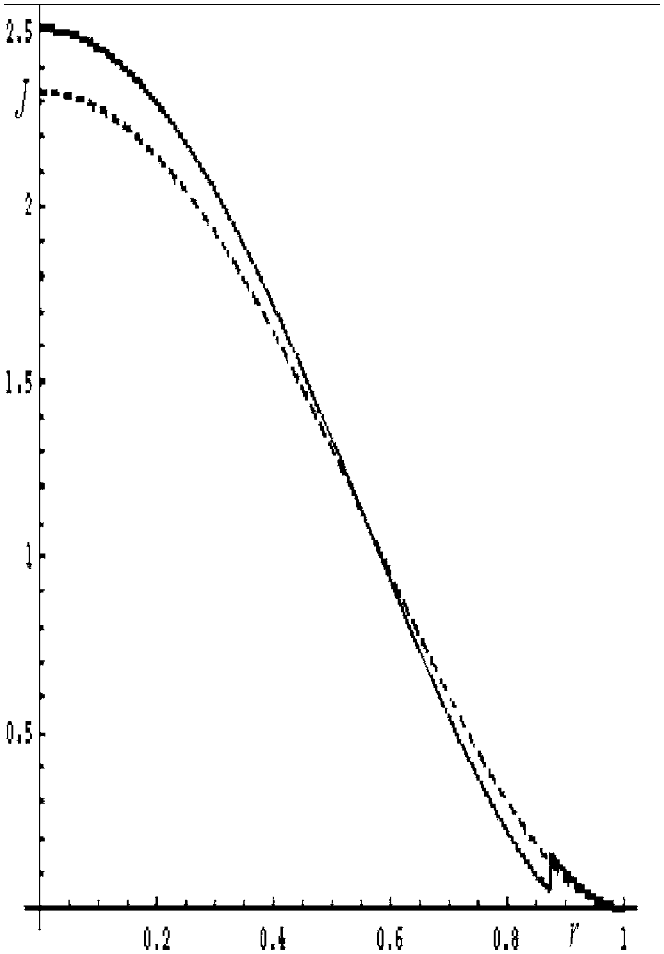

FIG. 5. The current density $J(r)$, dashed; and $J_f(r)$ solid curve; with $w=0.18$, in order to exaggerate the change. Note that the radius is normalized to the tokamak minor radius.

$$A = \lim\left[\frac{r\psi'_+}{\psi_+} + \frac{r\psi'_-}{\psi_-} - (a_+ + a_-)\ln\left|(r-r_s)/r_s\right|\right], \tag{D5}$$

where the subscripts + and − refer to $r>r_s$ and $r<r_s$, respectively, and the limit is $r\rightarrow r_s$ symmetrical about r_s. Since the value of Δ' in the initial equilibrium is small, of order $O(w)$, our main concern is with calculating how this changes in response to the island. We must therefore calculate a quantity $\Delta'(w)$ for the set of equilibria defined by Eqs. (D1) and (D2) above. Note that this bears no relation to the quantity sometimes used in discussions of nonlinear tearing modes, $\hat{\Delta}'(w)=[\psi'(r_s+w)-\psi'(r_s-w)]/\psi_0$. In the present calculation, $\Delta'(w)$ is obtained by the standard limiting process: $r\rightarrow r_s$. The functional dependence on w arises because we consider a set of equilibria which are parametrized by w. Before continuing with an example, we note that the discontinuities in these "cylindrical" equilibria are a convenient fiction. In fact, the island structure occupies the region around this apparent discontinuity and the perturbed linear eigenfunctions obtained from a solution of the tearing equation on either side of the resonance are matched to the nonlinear island solutions at values of $x \gg w$. In order to construct the matching function $M_{\text{outer}}(x)$ it is, however, convenient to analytically continue the functions $J_f(r)$ and $q_f(r)$ into the region which is, in reality, occupied by the island. The asymptotic form for the linear outer solution and for $M(x)$ can then be constructed in the region of interest, by making use of the standard linear tearing parameters Δ', A, a^+, and a^-. This method appears to be quite asymptotically rigorous but, like all asymptotic treatments, it may become very inaccurate as the small parameter (w in this case) is increased. If this turns out to be the case, a better method of constructing M_{out} (which does not make use of the analytic continuation into the island region) will be required.

As an example, we have constructed this quasi-cylindrical equilibrium and evaluated $\Delta'(w)$ and $A(w)$ for the case of an initial equilibrium with $J=J_0(1-r^2)^2$ and $q_0=0.86$. For this equilibrium, the $m/n=2/1$ mode is unstable with $\Delta'=0.33$. The results for $\Delta'(w)$ are shown in Fig. 4, from which it is clear that an accurate fit to the numerical data is given by

$$\Delta'(w) = 0.33 + 3.8w. \tag{D6}$$

The destabilization of the island by the thermal relaxation and by the current control system in this case can be understood from a comparison of the original and final current density profiles. These are shown in Fig. 5 [$J(r)$, dashed; $J_f(r)$ solid curve; with $w=0.18$, in order to make the change more evident]. The additional peaking of the final current profile has increased the current gradient for $r<r_s$, which is destabilizing. In addition, the axial value of the safety factor has dropped from $q_0=0.86$ to $q_0=0.80$, which could have implications for the $m=1$ sawtooth instability.

[1] H. P. Furth, J. Killeen, and M. N. Rosenbluth, Phys. Fluids **6**, 459 (1963).
[2] P. H. Rutherford, Phys. Fluids **16**, 1903 (1973).
[3] R. Fitzpatrick, Phys. Plasmas **2**, 825 (1995).
[4] C. C. Hegna and J. D. Callen, Phys. Fluids B **4**, 1855 (1992).
[5] F. Waelbroeck, J. W. Connor, and H. R. Wilson, Phys. Rev. Lett. **87**, 215003 (2001).
[6] M. Ottaviani, F. Porcelli, and D. Grasso, Phys. Rev. Lett. **93**, 075001 (2004).
[7] R. B. White, D. A. Monticello, M. N. Rosenbluth, and B. V. Waddell, Phys. Fluids **20**, 800 (1977).
[8] D. Biskamp, *Nonlinear Magnetohydrodynamics* (Cambridge University Press, Cambridge, UK, 1993).
[9] N. Louriero, S. C. Cowley, W. D. Dorland, M. G. Haines, and A. A. Schekochihin, Phys. Rev. Lett. **95**, 235003 (2005).
[10] D. F. Escande and M. Ottaviani, Phys. Lett. A **323**, 278 (2004).
[11] F. Militello and F. Porcelli, Phys. Plasmas **11**, L13 (2004).
[12] A. Thyagaraja, Phys. Fluids **24**, 1716 (1981).
[13] L. E. Zakharov, A. I. Smolyakov, and A. A. Subbotin, Sov. J. Plasma Phys. **16**, 451 (1990).
[14] A. Pletzer and F. W. Perkins, Phys. Plasmas **6**, 1589, (1999).
[15] R. J. Hastie, F. Militello, and F. Porcelli, Phys. Rev. Lett. **95**, 065001 (2005).
[16] F. Militello, G. Huysmans, M. Ottaviani, and F. Porcelli, Phys. Plasmas **11**, 125 (2004).
[17] G. Bertin, Phys. Rev. A **25**, 1786 (1982).
[18] R. D. Hazeltine, P. Helander, and P. Catto, Phys. Plasmas **4**, 2920 (1997).
[19] M. Kotschenreuther, R. D. Hazeltine, and P. J. Morrison, Phys. Fluids **28**, 294 (1985).
[20] C. C. Hegna, Phys. Plasmas **5**, 1767 (1998).
[21] H. Lutjens, J. F. Luciani, and X. Garbet, Plasma Phys. Controlled Fusion **43**, A339 (2001).
[22] N. Arcis, D. Escande, and M. Ottaviani, private communication (2005).
[23] D. Biskamp, Phys. Rep. **237**, 179 (1994).